AIP | Journal of Applied Physics

Defecting controllability of bombarding graphene with different energetic atoms via reactive force field model

Xiao Yi Liu, Feng Chao Wang, Harold S. Park, and Heng An Wu

Citation: J. Appl. Phys. **114**, 054313 (2013); doi: 10.1063/1.4817790
View online: http://dx.doi.org/10.1063/1.4817790
View Table of Contents: http://jap.aip.org/resource/1/JAPIAU/v114/i5
Published by the AIP Publishing LLC.

Defecting controllability of bombarding graphene with different energetic atoms via reactive force field model

Xiao Yi Liu,[1] Feng Chao Wang,[1] Harold S. Park,[2] and Heng An Wu[1,a)]
[1]*CAS Key Laboratory of Materials Behavior and Design, Department of Modern Mechanics, University of Science and Technology of China, Hefei, Anhui 230027, China*
[2]*Department of Mechanical Engineering, Boston University, Boston, Massachusetts 02215, USA*

(Received 4 June 2013; accepted 23 July 2013; published online 7 August 2013)

We study the bombardment of a suspended monolayer graphene sheet via different energetic atoms via classical molecular dynamics based on the reactive force field (ReaxFF). We find that the probability, quality, and controllability of defects are mainly determined by the impact site, the properties of the incident atom, and the incident energy. Through comparison with density functional theory calculations, we demonstrate that defects and vacancies in graphene form only in regions of sufficiently high electron density. Furthermore, the quality of defects is influenced by the bond order of the incident atom-carbon bonds, where a higher bond order leads to lower probability of pristine defects (vacancies) but a higher probability of direct-substitution. Finally, the incident energy plays an important role on the evolution and final pattern of defects in graphene. Based on the probability, quality, and controllability analysis performed, we depict a full-range energy spectrum for atomic bombardment, where we demonstrate that desirable defects such as single vacancies and direct-substitution can be created with the appropriate incident energy. [http://dx.doi.org/10.1063/1.4817790]

I. INTRODUCTION

Graphene has been studied intensely since its successful isolation from graphite in 2004 by Geim and his colleagues, due to its fascinating properties such as extremely high mobility, high elasticity, quantum electronic transport, and electromechanical modulation.[1–3] Defects and vacancies of graphene are ubiquitous,[4] which can change the mechanical,[5] electrical,[6] and magnetic[7,8] properties. While defects are typically viewed with concern as they generally decrease the strength of materials,[9] they can be beneficial for other applications involving sensors,[10] superconductors,[11,12] supercapacitors,[13,14] nanoelectronics,[15–17] and spintronics.[18–21]

Irradiation of ions,[22] electrons,[23,24] and atoms[25] on graphene is a general means to introduce defects and vacancies, which has been investigated in recent years. Specifically, the ability to control the number and types of defects is critical for etching or patterning graphene.[26–29] Methods to develop the controllability of bombardment have been proposed in both experiments and simulations. Wang *et al.*[28] demonstrated an efficient two-step process to dope graphene: create vacancies by high-energy atom/ion bombardment and fill these vacancies with the desired dopants. Krasheninnikov *et al.*[30–32] used standard molecular dynamics (MD) simulations to study the probability of substitution and defects. Pantelides *et al.*[33] studied high-energy ion (B and N) collisions with graphene fragments based on the time-dependent density functional theory (TDDFT). However, these previous studies focused mainly on bombarding graphene with a specific projectile, while focusing on the effects of varying the incident energy. Therefore, the effects of the impact site and the properties of the projectile, and specifically its reactivity with graphene, remain unresolved.

In the bombarding process, the three key issues to understand are the probability, quality, and controllability of the resulting defects.[28,30,32,33] Although the bombardment process can be studied experimentally, it is difficult to obtain the details of the bombarding process and specifically the process of defect creation due to issues in time-resolution. Hence, atomistic simulation is an effective way to answer these three questions.

Standard MD and TDDFT methods have been used to study the bombardment of graphene.[32,33] Using standard MD simulations, the final patterns of defects and vacancies can be obtained. However, the information obtained regarding bonding, debonding, and defect creation is questionable due to the fact that the interatomic potentials that have been utilized do not account for the chemistry involved in bond breaking and creation. These issues can be captured using TDDFT, but the final defect patterns may not be accurate due to time and length scale issues inherent to quantum mechanics simulations.

Therefore, we use the reactive force field potential (ReaxFF)[34] to study the bombardment of graphene via different energetic atoms, where ReaxFF is used to describe the carbon-carbon and carbon-projectile interactions. To achieve proper dissociation of bonds to separated atoms, the relationship between bond distance and bond order, as well as the relationship between bond order and bond energy, is used in ReaxFF. The accuracy of simulation results using ReaxFF is comparable to that of a quantum mechanics approach, though with much lower computational expense.[35,36] In this work, we used the Fe/C,[37] Au/C,[38,39] and O/C (Ref. 40)

a)Author to whom correspondence should be addressed. Electronic mail: wuha@ustc.edu.cn

reactive force fields to simulate the bombardment of a suspended graphene monolayer with different energetic atoms.

Through this study, we have identified the main factors controlling the three concerns discussed above (probability, quality, and controllability of the resulting defects). Specifically, by investigating the effects of the impact site, the carbon-bombarding atom interaction energy as well as the incident energy of the bombarding atom, we discuss the initiation, evolution, and eventual final pattern of defects and vacancies. Finally, a full-range energy spectrum of incident atoms is depicted, and differences in the energy spectrum for different projectiles are discussed. By comparing the energy spectrum for the three atoms, general rules are given to develop controllable techniques for defect generation. Finally, we show that specific defects or substitutions can be controllably achieved within a specific incident energy range, which is crucial for controllable patterning or etching processes in graphene.

II. PROBLEM OVERVIEW AND SIMULATION METHODS

A schematic of the simulation setup used in the present work is shown in Figure 1. The publicly available, Sandia-developed simulation code LAMMPS[41] was used for all MD simulations. The target graphene monolayer simulated in this work consisted of up to 3000 ReaxFF atoms, while the boundaries of the monolayer were not constrained. The initial graphene configuration was obtained by relaxing the monolayer at 300 K (for 10 ps) within an NVT ensemble (The number of particles (N), the volume (V) and the temperature (T) in the ensemble are constant, also referred as canonical ensemble). The timestep is set as 0.1 fs, which is sufficiently small to resolve the details of bonding, debonding, and charge variation in collision.[37–40] Collisions between the incident projectile and graphene were simulated within an NVE ensemble (The number of particles (N), the volume (V) and the energy (E) in the ensemble are constant, also referred as microcanonical ensemble.) for up to 1.5 ps in order to allow completion of the collision process. Following the collision, a dynamic relaxation period of 4 ps was observed within an NVT ensemble to achieve equilibrium in the graphene after the collision and to obtain the final defect pattern. Visualization of the entire process was performed using Atomeye.[42]

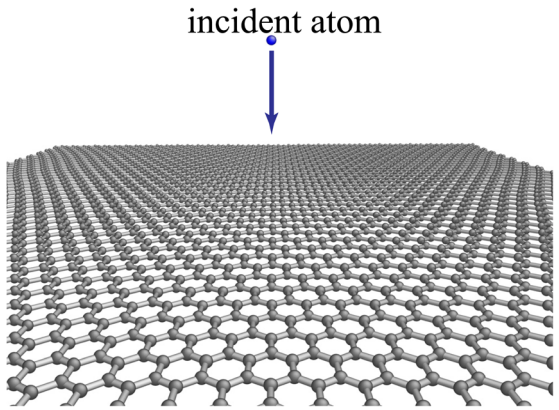

FIG. 1. Schematic representation of the simulated bombardment process.

One general issue to address before discussing the key findings is that if the incident atom cannot penetrate through the graphene monolayer, functionalized graphene will form, where this is typically considered a contamination.[28,30,32] Because functionalized contamination is undesirable and because an energy transfer of at least 20 eV is required to displace a carbon atom in a graphitic structure,[2] the lowest kinetic energy of the incident atom considered in this work is 10 eV. To study the effect of different atom types, Au, Fe, and O atoms were used as the incident projectile atoms.

III. EFFECT OF IMPACT SITES ON THE PROBABILITY OF DEFECT CREATION

Krasheninnikov *et al.*[30,32] discussed the relationship between the probability of defect creation and the incident energy. However, that study did not connect the probability of defect creation with the impact sites on the graphene monolayer. To simplify the discussion of the relationship between the probability of defect creation and the impact site, we first study the bombardment of graphene by a specific projectile with a specific incident energy, while the variations due to different incident energies and projectile types will be discussed later. To ensure that the projectile penetrates through the target graphene monolayer, we use a Fe projectile with an incident energy of 100 eV.

As shown in Figure 2(a), we consider a rectangular unit cell containing a single graphene hexagon and mesh it into a 51×51 grid containing 2601 grid points. To simulate all possible impact sites, we perform a simulation of bombarding at each grid point, where statistics regarding the escape of carbon atoms from the hexagon are shown in Figure 2(c) in contour form. Although the types of defects and vacancies are not revealed in Figure 2(c), it is clear that any single vacancies (SV), double vacancies (DV), or multi-vacancies (MV) that form will occur in a specific area, i.e., immediately surrounding one of the original carbon atom lattice sites. Furthermore, as shown in Figure 2(b), a stable bond vacancy can form in cases corresponds to a head-to-bond impact where the bond connecting two carbon atoms is bisected by the incident projectile, resulting in destruction of the corresponding C-C bond. This phenomenon has not been observed in previous MD simulations, although it has been seen in TDDFT simulations.[33]

Similar contour plots can be obtained for Au and O projectiles. Furthermore, the probability of SV increases for low incident energies but decreases for high incident energies, where the variation in the probability of a SV does not vary monotonically with the incident energy. In contrast, the probability of a DV or MV is low for higher incident energies, and nearly zero for lower energies. This relationship between incident energy and defect creation probability is consistent with the work of Krasheninnikov *et al.*[30,32] Furthermore, comparing the contour map in Figure 2(c) with the DFT calculation shown in Figure 2(d), we find that defects and bond-vacancies can only form in areas with an electron density over $1.5e^{-}$. In these areas, high electron

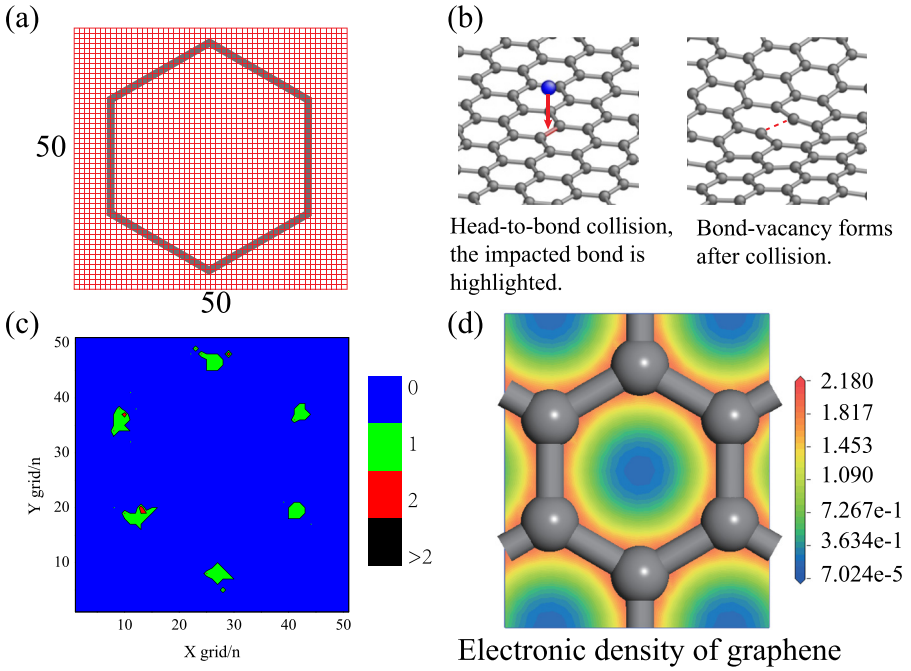

FIG. 2. (a) Rectangular unit cell containing 51×51 mesh and single hexagon of carbon atom. Every grid point is an impact site. (b) Head-to-bond collision, where a stable bond-vacancy can be formed without losing any carbon atoms. (c) The contour plot of the numbers of lost carbon atoms across the whole grid domain. (d) The contour plot of electron density distribution.

density implies a strong interaction between the carbon atoms and the projectile, and thus the covalent sp^2 C-C bonds can be destroyed only with strong interaction.

While the impact site cannot be controlled precisely in experiments, Figure 2(c) makes clear that bombarding graphene at most points will not introduce defects or vacancies due to the low electron density at most points in the graphene monolayer; this result implies that continuous bombardment should be viable as a technique to induce defects in graphene.

Before moving forward, we note that the impact site does play an important role in the probability of creating defects and vacancies. Based on the ReaxFF-based MD simulations in conjunction with our DFT results, head-to-hexagon bombarding, in which an incident atom impacts the center of an individual hexagon, introduces few defects. Therefore, we focus upon head-to-head and head-to-bond collisions in Secs. IV and V to investigate the controllability of the resulting defects.

IV. EFFECT OF PROJECTILE PROPERTIES ON THE QUALITY OF DEFECTS

The quality of the introduced defects is another crucial parameter for techniques to introduce defects in graphene via bombardment.[28,31] Here, we define higher quality to mean clean defects (vacancies) without the introduction of disarray of contamination in the region neighboring the impact site. To determine the main factors influencing the quality of defects and vacancies, we simulate head-to-bond and head-to-head collisions with different projectiles.

For head-to-bond collisions, the bonding and debonding processes are found to be remarkably different for different projectiles, which we elucidate via MD simulations using ReaxFF, as summarized in Table I for Fe, Au, and O atoms. Using ReaxFF, we can determine whether the process of bond breaking is physical or chemical by considering the maximum variation of charge, the number of bonding carbon atoms, and the bond order, where for reference we note that the C-C bond order is about 1.300. The bond order is a distance-dependent function in ReaxFF, which is used to represent the contributions of chemical bonding to the potential energy. This quantity can be obtained as an output from the ReaxFF simulations.

Because there is essentially no charge transfer between Au and C atoms during the bombardment, this interaction (Au atoms breaking a C-C bond) is considered a physical process. In contrast, charge is transferred in the interactions between C-O and C-Fe, which indicates that a chemical process occurs for those interactions. Furthermore, the bond order of C-O is much higher than that of Fe-C, which means that the C-O bond is much stronger than the Fe-C bond.

This bond strength plays an important role when the incident projectile is escaping from the target graphene monolayer after the collision, which occurs via the breaking of bonds between the incident projectile atom and the carbon atoms in the graphene monolayer. Specifically, as illustrated in Figure 3, for the bond breaking process due to a head-to-bond collision, stronger bond results in the dragging of C atoms as the incident atom moves through the graphene monolayer. Furthermore, because the C-O bond strength is greater than C-Fe, more C atoms are dragged by the O atom, which results in more disorder in graphene bombarded with O and a higher quality of defect in graphene bombarded with Fe.

TABLE I. Bonding information related to C-energetic atom collision from the ReaxFF potential model.

Projectile	Maximum variation of charge/e$^-$	Average bond order	Number of bonding carbon atoms	Strength of chemical interaction
O	−0.3	2.737	2	Strong
Fe	+0.5	0.305	6	Medium
Au	∼0	∼0	0	Weak

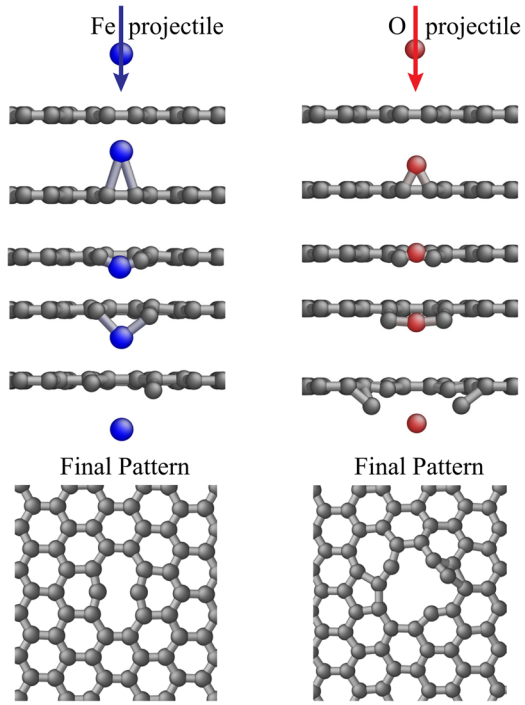

FIG. 3. Quality of resulting defects due to various degrees of atom-drag induced by (left) incident Fe projectile; (right) incident O projectile. Both projectiles have an incident energy of 100 eV, and both projectiles impact the graphene monolayer via a head-to-bond collision.

In contrast, atom-drag decreases the quality of the defects and vacancies, and it increases the probability of random vacancies and defects. Strong bonds between the projectile and the carbon atoms can also increase the critical energy needed for the projectile to penetrate through the target sheet, which plays an important role in energy transfer between incident and target atoms. The critical incident energy needed for an O atom to penetrate the graphene monolayer in a head-to-bond collision is much higher than that of other collisions due to atom-drag.

Bond strength also plays an important role in head-to-head collisions. Because the new bonds will not form before the projectile impacts the graphene monolayer, atom-drag does not occur due to the weak interactions prior to impact between the projectile and the neighboring carbon atoms. Instead, direct-substitution can be observed. If the incident atom is the desired atom with which to dope graphene, this is useful.[19] Otherwise, the substitution is not preferred.[28] Substitutions are observed for Fe and O projectiles, but not for the Au projectile. This is because for Fe and O, bonds between the projectile and neighboring carbon atoms form, which reduces the kinetic energy of the projectile and results in substitutions for those atoms in place of the original carbon atoms. In contrast, due to the physical nature of bonding between Au and carbon, Au projectiles will either attach to the graphene sheet for low incident energies or bounce back or penetrate the target sheet for higher incident energies, which is consistent with the previous experiments.[28]

However, once the incident atom has substituted for the carbon atom in the graphene monolayer, it does interact with the neighboring carbon atoms in the hexagonal unit cell ring. For Fe and O, bonds between projectile and neighboring carbon atoms form, and they highly decrease the kinetic energy of projectile. New bonds between projectile and neighboring carbon atoms facilitate direct-substitution.

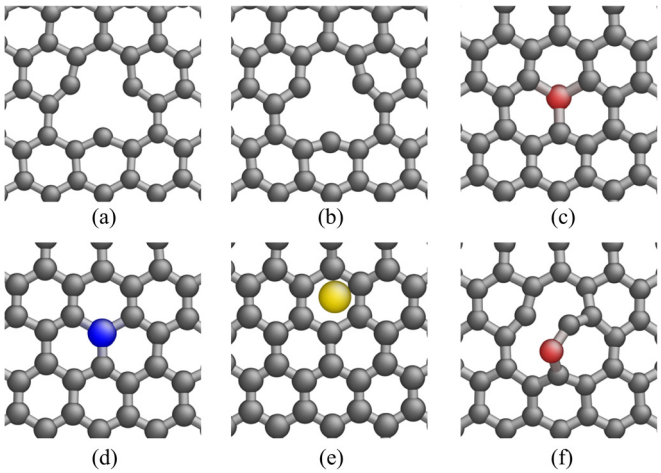

FIG. 4. Defect pattern induced by head-to-head collisions: (a)–(c) Fe/Au/O projectiles with incident energy of 100 eV; (d) substitution of Fe projectile with incident energy of 60 eV. (e) Au atom attaches with graphene sheet with low incident energy of 20 eV. (f) O atom bonds with graphene sheet with low incident energy of 25 eV.

We illustrate the nature of head-to-head collisions in Figure 4, which shows head-to-head collisions with the same incident kinetic energy of 100 eV for Fe, Au, and O projectiles. Direct-substitution is only observed in bombardment of O projectile. By decreasing the incident energy of the Fe projectile, direct-substitution happens starting at an incident energy of 60 eV as shown in Figure 4(d). However, the substitution is not observed for Au projectile with decreasing incident energy. When the incident energy decreases to 20 eV, Au contamination is formed, as shown in Figure 4(e), where the Au atom can randomly walk on the target sheet without bonds. While O forms a direct substitution at an incident energy of 100 eV, as the incident energy is lowered to around 20 eV, the O projectile forms stable functionalized contamination bonding with carbon atoms in the graphene as shown in Figure 4(f).

Overall, this analysis shows that the quality of defects and vacancies are strongly influenced by the bond strength between the projectile and carbon atoms. Strong bonds do not lead to pristine defects or vacancies due to atom-drag; however, stronger bonding does increase the probability of direct-substitution.

V. ENERGY SPECTRUM OF THE RESULTING DEFECTS FOR Au/Fe/O PROJECTILES

As discussed above, the incident energy plays an important role in defecting probability and controllability. We find that the impact site and properties of projectiles also play important roles, which have not been elucidated in previous study.[28,30–33,43] We have shown that the probability of defects is mainly influenced by impact site, while the quality of defects is mainly influenced by interactions between projectile and carbon atoms.

We have performed comprehensive simulations for three projectiles (Au, Fe, and O), three impacting sites

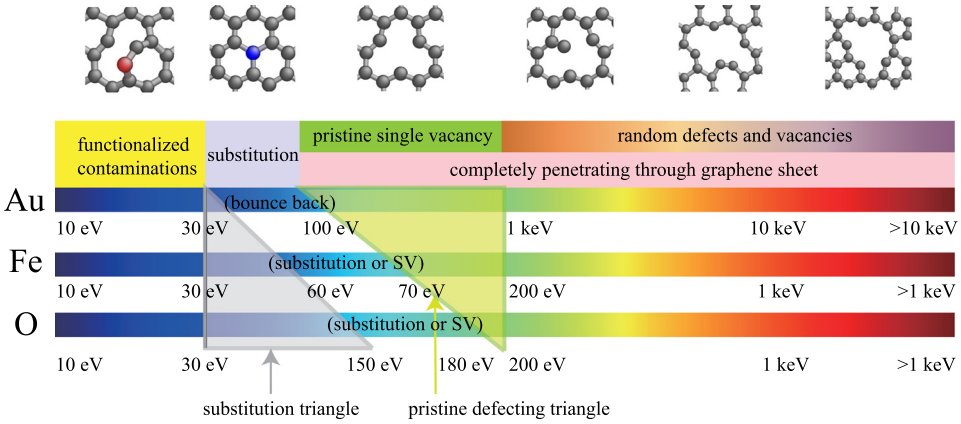

FIG. 5. Energy spectrum that relates resulting defect type to the incident energy for Au, Fe, and O projectiles.

(head-to-head, head-to-bond, and head-to-hexagon), and incident energy ranging from 10 eV to a few keV. For each simulation, the possible initiation and evolution pattern of defects are observed. To summarize these results, an energy spectrum of projectiles is depicted, as shown in Figure 5.

The Au, Fe, and O projectiles are ordered from top to bottom by strength of chemical interactions, as listed in Table I. Generally, these projectiles have similar stages in the spectrums of incident energy. If the incident energy is smaller than a critical value, the projectile cannot penetrate through the graphene sheet and finally becomes a functionalized contaminant on the graphene surface. The substitution band appears with increasing incident energy, where a substitution corresponds to the replacement of a carbon atom with the incident projectile. The single vacancy band follows with further increasing incident energy. In this energy range, the probability of obtaining a pristine single vacancy is guaranteed. When the incident energy is larger than another critical value, single vacancies, double vacancies, and multi-vacancies appear, but they are random in this band. This energy spectrum is consistent with experiments of Wang *et al.*[28] and simulations of Krasheninnikov *et al.*[44]

Figure 5 shows that Au, Fe, and O (except for head-to-bond collisions for O due to the strong atom-drag mechanism discussed previously) all require about 30 eV in order to penetrate the graphene monolayer. The largest differences between the defects induced by the various projectiles are in the substitution and pristine single vacancy bands, where the bands for each defect are shown using the shaded triangles in Figure 5. Specifically, the width of the substitution band increases while the width of the pristine single vacancy band decreases with increasing strength of chemical interaction between the projectile and the incident carbon atoms. The substitution triangle trend can be explained by the fact that strong bonds between the projectile and the neighboring carbon atoms facilitate direct-substitution as analyzed above. In contrast, because the strong bonds between the projectile and carbon atoms decrease the defect quality, the weaker chemical interactions between the projectile and the carbon atoms lead to a wider band for pristine single vacancies. We feel this result (the triangle-band features in the energy spectrum) should be of particular experimental relevance as substitutions and pristine single vacancies are the most important and desirable for controllable defect patterning.

VI. CONCLUSIONS

In this work, we utilized classical molecular dynamics simulations and a reactive force field to study the effects of the impact site, the properties of the incident projectile, and the incident energy on the resulting defect structure of bombarded monolayer graphene. In doing so, we have been able to elucidate and clarify the issues controlling defect quality, controllability, and probability. First, the probability of creating a defect in the graphene monolayer is mainly influenced by the impact site, where defects and vacancies are most likely to form when the impact site lies in an area with a sufficiently large electron density, found to be over $1.5e^{-}$ in this work. While the impact sites cannot be precisely controlled in experiments, we have found that impact at sites with low electron density will not introduce vacancies or defects, which implies that continuous bombardment is a feasible experimental technique for generating defects in graphene. Second, the quality of defects and vacancies is controlled by the interaction and physicochemical nature of bonding between the projectile and the carbon atoms. Stronger bonds between the projectile and carbon lead to a higher probability of substitution but lower quality of defects due to the dragging of neighboring atoms. Third, the controllability is different for different energy bands. In the substitution band and the single vacancy band, the specific defect (substitution or single vacancy) can be achieved with guaranteed probability and quality. The length of the substitution band increases with increasing strength of chemical interaction, while the length of the pristine single vacancy band decreases. At higher impact energies, double and multi-vacancies typically form with poor controllability. Finally, we have presented an energy spectrum relating the properties and incident energies of the projectiles to the resulting defects, which should prove valuable to experimentalists in choosing a proper projectile with appropriate incident energy to achieve the desired defect structure in the bombarded graphene monolayer.

ACKNOWLEDGMENTS

This work was supported by National Science Foundation of China (11172289 and U1262103).

[1]A. K. Geim, Science **324**, 1530 (2009).
[2]A. K. Geim and K. S. Novoselov, Nat. Mater. **6**, 183 (2007).

[3]K. S. Novoselov, A. K. Geim, S. V. Morozov, D. Jiang, Y. Zhang, S. V. Dubonos, I. V.Grigorieva, and A. A. Firsov, Science **306**, 666 (2004).
[4]A. Ferreira, X. F. Xu, C. L. Tan, S. K. Bae, N. M. R. Peres, B. H. Hong, B. Ozyilmaz, and A. H. C. Neto, EPL **94**, 28003 (2011).
[5]R. Grantab, V. B. Shenoy, and R. S. Ruoff, Science **330**, 946 (2010).
[6]J. M. Carlsson and M. Scheffler, Phys. Rev. Lett. **96**, 046806 (2006).
[7]E. J. G. Santos, D. Sanchez-Portal, and A. Ayuela, Phys. Rev. B **81**, 125433 (2010).
[8]G. Khurana, N. Kumar, R. K. Kotnala, T. Nautiyal, and R. S. Katiyar, Nanoscale **5**, 3346 (2013).
[9]R. Jack, D. Sen, and M. J. Buehler, J. Comput. Theor. Nanosci. **7**, 354 (2010).
[10]F. Schedin, A. K. Geim, S. V. Morozov, E. W. Hill, P. Blake, M. I. Katsnelson, and K. S. Novoselov, Nat. Mater. **6**, 652 (2007).
[11]J. H. Chen, L. Li, W. G. Cullen, E. D. Williams, and M. S. Fuhrer, Nat. Phys. **8**, 353 (2012).
[12]H. B. Heersche, P. Jarillo-Herrero, J. B. Oostinga, L. M. K. Vandersypen, and A. F. Morpurgo, Nature (London) **446**, 56 (2007).
[13]X. J. Lu, H. Dou, B. Gao, C. Z. Yuan, S. D. Yang, L. Hao, L. F. Shen, and X. G. Zhang, Electrochim. Acta **56**, 5115 (2011).
[14]M. D. Obradovic, G. D. Vukovic, S. I. Stevanovic, V. V. Panic, P. S. Uskokovic, A. Kowal, and S. L. Gojkovic, J. Electroanal. Chem. **634**, 22 (2009).
[15]D. S. Yu, L. Wei, W. C. Jiang, H. Wang, B. Sun, Q. Zhang, K. L. Goh, R. M. Si, and Y. Chen, Nanoscale **5**, 3457 (2013).
[16]M. Giovanni, H. L. Poh, A. Ambrosi, G. J. Zhao, Z. Sofer, F. Sanek, B. Khezri, R. D. Webster, and M. Pumera, Nanoscale **4**, 5002 (2012).
[17]O. Glukhova and M. Slepchenkov, Nanoscale **4**, 3335 (2012).
[18]F. Cervantes-Sodi, G. Csanyi, S. Piscanec, and A. C. Ferrari, Phys. Rev. B **77**, 165427 (2008).
[19]A. V. Krasheninnikov, P. O. Lehtinen, A. S. Foster, P. Pyykko, and R. M. Nieminen, Phys. Rev. Lett. **102**, 126807 (2009).
[20]O. V. Yazyev and L. Helm, Phys. Rev. B **75**, 125408 (2007).
[21]S. N. Wang, R. Wang, X. W. Wang, D. D. Zhang, and X. H. Qiu, Nanoscale **4**, 2651 (2012).
[22]D. C. Bell, M. C. Lemme, L. A. Stern, J. Rwilliams, and C. M. Marcus, Nanotechnology **20**, 455301 (2009).
[23]M. D. Fischbein and M. Drndic, Appl. Phys. Lett. **93**, 113107 (2008).
[24]W. P. Zhu, H. T. Wang, and W. Yang, Nanoscale **4**, 4555 (2012).
[25]M. C. Lemme, D. C. Bell, J. R. Williams, L. A. Stern, B. W. H. Baugher, P. Jarillo-Herrero, and C. M. Marcus, ACS Nano **3**, 2674 (2009).
[26]S. Akcoltekin, H. Bukowska, T. Peters, O. Osmani, I. Monnet, I. Alzaher, B. B. d'Etat, H. Lebius, and M. Schleberger, Appl. Phys. Lett. **98**, 103103 (2011).
[27]B. Song, G. F. Schneider, Q. Xu, G. Pandraud, C. Dekker, and H. Zandbergen, Nano Lett. **11**, 2247 (2011).
[28]H. T. Wang *et al.*, Nano Lett. **12**, 141 (2011).
[29]A. R. Botello-Mendez, X. Declerck, M. Terrones, H. Terrones, and J. C. Charlier, Nanoscale **3**, 2868 (2011).
[30]E. H. Ahlgren, J. Kotakoski, and A. V. Krasheninnikov, Phys. Rev. B **83**, 115424 (2011).
[31]A. V. Krasheninnikov and K. Nordlund, J. Appl. Phys. **107**, 071301 (2010).
[32]O. Lehtinen, J. Kotakoski, A. V. Krasheninnikov, A. Tolvanen, K. Nordlund, and J. Keinonen, Phys. Rev. B **81**, 153401 (2010).
[33]S. Bubin, B. Wang, S. Pantelides, and K. Varga, Phys. Rev. B **85**, 235435 (2012).
[34]A. C. T. van Duin, S. Dasgupta, F. Lorant, and W. A. Goddard, J. Phys. Chem. A **105**, 9396 (2001).
[35]S. S. Han, J. K. Kang, H. M. Lee, A. C. T. van Duin, and W. A. Goddard, J. Chem. Phys. **123**, 114703 (2005).
[36]K. D. Nielson, A. C. T. van Duin, J. Oxgaard, W. Q. Deng, and W. A. Goddard, J. Phys. Chem. A **109**, 493 (2005).
[37]M. Aryanpour, A. C. T. van Duin, and J. D. Kubicki, J. Phys. Chem. A **114**, 6298 (2010).
[38]T. T. Jarvi, A. C. T. van Duin, K. Nordlund, and W. A. Goddard, J. Phys. Chem. A **115**, 10315 (2011).
[39]J. A. Keith, D. Fantauzzi, T. Jacob, and A. C. T. van Duin, Phys. Rev. B **81**, 235404 (2010).
[40]K. Chenoweth, A. C. T. van Duin, and W. A. Goddard, J. Phys. Chem. A **112**, 1040 (2008).
[41]S. Plimpton, J. Comput. Phys. **117**, 1 (1995).
[42]J. Li, Modell. Simul. Mater. Sci. Eng. **11**, 173 (2003).
[43]S. G. Srinivasan and A. C. T. van Duin, J. Phys. Chem. A **115**, 13269 (2011).
[44]T. Susi *et al.*, ACS Nano **6**, 8837 (2012).